0038-075x/94/1573-0129$03.00/0
SOIL SCIENCE
Copyright © 1994 by Williams & Wilkins

March 1994
Vol. 157, No. 3
Printed in U. S. A.

STEADY-STATE INFILTRATION AS A FUNCTION OF MEASUREMENT SCALE[1]

P. J. SHOUSE,[2] T. R. ELLSWORTH,[3] AND J. A. JOBES[2]

Steady-state infiltration rates were measured at three instrument scales within a 4.0 x 4.0-m field plot. The three scales were 4.0 × 4.0 m (scale S_L, $n = 1$), 1.0 x 1.0 m (scale $S_{L/4}$, $n = 16$), and 0.25 x 0.25 m (scale $S_{L/16}$, $n = 256$). After a 30-day ponding period under a constant hydraulic head, infiltration measurements were made at each measurement scale. Even though the entire area was sampled at each instrument scale, the average infiltration rate decreased with decreasing size of infiltrometer. The infiltration rate measurements were adjusted assuming an "apparent" stagnation zone of 4 cm along the boundaries of each infiltrometer. This adjustment produced average infiltration rates of 1.96 cm/h for each of the smaller measurement scales. This value was in excellent agreement with the final value measured at scale S_L upon completion of the experiment (1.97 cm/h). However, the value for the "apparent" stagnation zone was found to be valid only in an average sense, because the correlation between the adjusted average value of the $S_{L/16}$ measurements and the adjusted value of the $S_{L/4}$ measurements was not significant. The 256 measurements at scale $S_{L/16}$ were neither normal nor lognormally (natural log (In)) distributed, although the latter provided a somewhat better representation. Too few measurements were available to determine the probability distribution for scale $S_{L/4}$. The regularized semivariogram (range of 0.7 m) for scale $S_{L/16}$ was deconvoluted to provide estimates of the point semivariograms for both the actual and adjusted measurement scales, leading to spatial ranges of 0.21 and 0.30 m for actual and adjusted, respectively. With or without adjustment, dispersion variance analyses illustrated that the spatial structure estimate obtained from measurement scale $S_{L/16}$ was inconsistent with that obtained from measurement scale $S_{L/4}$. Thus, we conclude that the infiltrometer instrument fundamentally alters the infiltration process in such a way that measurements are only meaningful in a relative sense.

1 Joint contribution of the USDA, ARS U.S. Salinity Laboratory, and the Dept. of Agronomy, Univ. of Illinois.

2 USDA, ARS, U.S. Salinity Laboratory, Riverside, CA 92501.

3 Dept. of Agronomy, University of Illinois, Urbana, IL 61801.

Received Feb. 8, 1993; accepted Sept. 2, 1993.

During the past two decades, considerable research has focused on characterizing the spatial variability of hydraulic properties in natural porous media (see reviews by Jury 1985 and Gelhar et al. 1992). As a result, it has become apparent that the measurement method used to quantify a spatially variable soil property has significant impact on the observed quantity. The implicit heterogeneity present in the spatial region of interest is represented explicitly via the measurement device and methodology.

Sisson and Wierenga (1981) studied the spatial variability of steady-state infiltration rates using three different sizes of infiltrometers. They observed that the underlying statistical distribution changed as a function of measurement scale. A similar observation with respect to sorptivity was observed by Clothier and White (1981). They found that the frequency distribution changed with measurement scale, and the variance decreased with increasing scale. However, as noted by White (1988), variance has also been observed to increase with measurement scale. Thus spatial variance structure is quite complex and does not necessarily adhere to either the assumptions of ergodicity and stationarity or the concept of representative elementary volume.

Saturated hydraulic conductivity measurements using both permeameters and flowmeter tests indicate that instrument type may influence the estimation of spatial correlation structure (Hess et al. 1992). In another study, Zobeck et al. (1985) measured saturated hydraulic conductivity using constant and falling head permeameter methods on three different cross-sectional areas of "undisturbed" soil samples col-

lected from two different soil types. Their results suggest that the influence of measurement methodology on spatial variability estimation (mean and variance in their case) is soil-dependent as well. Lauren et al. (1988) measured the soil-saturated hydraulic conductivity using various size samples in situ and in the laboratory. They concluded that the description of the correlation scale was influenced by both sample size and measurement method.

Clothier (1988) points out the cyclic and iterative interplay between theory and experiment that leads to continuous refinement of measurement devices and methods. The infiltrometer is the most common device used to characterize infiltration in situ, and general guidelines for its use are provided by Bouwer (1986). According to the general guidelines, an infiltrometer should have appropriate size and a constant head of water in order to minimize lateral divergence of flow caused by gradients of hydraulic pressure and edge effects. Also, an infiltrometer should be inserted with minimum soil disturbance. Our study was designed to observe the effects of infiltrometer size on steady-state infiltration rate in a sandy loam soil. Our secondary purpose was to qualitatively observe the effect of insertion depth on infiltration rate.

MATERIALS AND METHODS

The site chosen for the study was an experimental plot that has been in use for approximately 30 years for salt tolerance studies at the U.S. Salinity Laboratory in Riverside, CA. The plot was 4.0 x 4.0 m in size and was surrounded by concrete wall borders that extended 0.25 m above the plot surface and 1.0 m below the surface. The soil was Pachappa sandy loam (mixed, thermic, Mollic Haploxeralf) and was homogenous with respect to particle size distribution to a depth of 2 m.

A neutron access tube was installed in the center of the plot to a depth of 2.0 m. Tensiometers, one at each of 10 depths (0.2 to 2.0 m, every 0.2 m), were located at equi-spaced intervals on the circumference of a 0.5-m diameter circle around the access tube. A constant head of water (0.1 m) was ponded on the plot surface for 30 days immediately before the study. Daily measurements of flow into the plot during this 30-day period as well as neutron probe and tensiometer readings showed that steady-state had been attained after approximately 10 days. The steady-state flow rate into the entire 4.0 x 4.0-m plot was measured both before and after the experiment with a float valve and calibrated water flow meter.

Two infiltrometers were built using 16-gauge galvanized steel. The dimensions of the first were 1.0 x 1.0 x 0.3 m. The second was a four-cell infiltrometer with outside dimensions of 1.0 x 0.25 x 0.30 m, giving the dimensions of each cell as 0.25 x 0.25 x 0.30 m. A large plastic barrel placed on a balance, provided the water supply to the 1.0-m infiltrometer. A float valve inside the infiltrometer was used to maintain a constant head. The water level in the 0.25-m infiltrometers was controlled using four mariotte syphon tubes (Bouwer 1986) built using 2.0 m long, 0.062 m diameter plexiglass. Flow rates were measured using a graduated scale (cm) attached to the side of each syphon tube. Infiltrometers were installed to a depth of 0.10 m using a vibrating hammer. Based on preliminary studies near the site, installation with the vibrating hammer gave a much smoother and more continuous force compared with the traditional method of raising and dropping a weight (Bouwer 1986). A network of catwalks, which spanned the experimental plot eliminating compaction by foot traffic, was used.

During the entire study period, a 0.1-m constant head was maintained on the 4.0 x 4.0-m plot. In order to determine the effect of installing the infiltrometers on the steady-state flow rate, infiltration was measured in 15-min intervals over an 8-h period. Infiltration rates did not change after the first 15 min following installation of either infiltrometer, indicating that flow rapidly resumed steady-state. Thus, after the disturbance of driving infiltrometers into the soil at each subplot, a l-h waiting period was employed before monitoring the final flow rate. The steady-state flow rate was then taken as the average flow rate in the subsequent hour following this waiting period. The first measurement taken was with the 1.0-m infiltrometer placed near the center of the plot. After measurements were made, the infiltrometer was removed, leaving an impression in the soil. This impression provided a guide for the 0.25-m infiltrometer. The installation and measurement methods used with both infiltrometers were identical. After the 16 0.25-m infiltrometer measurements were made within a specified 1-m^2 subplot, the 1.0-m infiltrometer was installed in a section

adjacent to the preceding location and the entire procedure repeated. This procedure was continued until the steady-state infiltration rate on the 16 1.0 x 1.0-m subplots and the 256 0.25 × 0.25-m sub-subplots had been measured. As noted above, after completion of all measurements, the steady state infiltration rate into the 4.0 x 4.0-m plot was again measured.

RESULTS AND DISCUSSION

Process description

The flow within the 4.0 x 4.0-m plot was at steady-state 20 days before taking the infiltration rate measurements, and was determined to be 2.0 cm/h. In addition, hydraulic gradient and water content were constant, within experimental error, to a depth of 2.0 m during the entire experiment. Infiltration measurements were taken over a 10-day period. After completing the infiltration experiment, we measured the flow rate on the entire 4.0 x 4.0-m plot again and determined it to be 1.97 cm/h. These conditions satisfy a special case of the Richards' Equation for steady saturated flow (Sposito 1986), at least for the upper 1.0 m of the soil profile, the depth of the concrete plot borders. In this spatial domain, the saturated hydraulic conductivity tensor is appropriate, and the water flux density vector, q(x,y,z) is not a function of time. The governing equation for spatially heterogenous saturated medium is thus:

$$q = -K_s \cdot \nabla H, \qquad (1)$$

where K_s is the saturated hydraulic conductivity tensor, and H is the total hydraulic head, assumed to consist entirely of gravity and hydrostatic pressure for our experimental conditions.

Scale *dependence of the mean infiltration rate*

The methods used in this experiment provided three scales of observation, S_L = 4.0 x 4.0 m, $S_{L/4}$ = 1.0 x 1.0 m, and $S_{L/16}$ = 0.25 x 0.25 m. Table 1 summarizes the average steady-state infiltration rate, (R), measured at each scale. The skewness and variance for $S_{L/16}$ and $S_{L/4}$ are also given; a positive skewness implies the existence of extremely large values. The mean infiltration rate for scale S_L was 2.00 cm/h, being the average of the before (2.04) and after (1.97) steady-state measurements on the entire 4.0 X 4.0-m plot. The apparent mean infiltration rate decreased with decreasing scale (Table 1).

TABLE 1

Statistics of the steady-state (<R>) *infiltration rates* at *each measurement scale*

Measurement scale (m)	Mean (cm/h)	Variance ([cm/h]²)	Skewness
4.0 x 4.0 (SL) (n = 1)	2.00	nd	nd
1.0 x 1.0 (SL/4) (*n* = 16)	1.66	0.36	1.40
0.25 x 0.25 (SL/16) (*n* = 256)	0.91	0.37	3.68

nd indicates insufficient data.

All three measurement scales encompassed the same spatial domain, and care was taken to ensure observations corresponded to steady flow; hence, the decreasing mean infiltration rate with decreasing measurement scale cannot be explained by reason of lateral divergence of flow below the 1.0-m deep concrete border. The only experimental difference between the several scales of observation was the number of metal borders (infiltrometers) inserted into the plot to measure the intake rate. Since the order of measurement was 4.0 X 4.0 m, 1.0 × 1.0 m, and 0.25 x 0.25 m, it is evident that mean water flow decreases with an increasing number of metal borders inserted into the plot. This was not a permanent condition because the before and after measurements at the 4.0 X 4.0-m scale were practically the same.

We are quite confident that lateral divergence of flow at the bottom of the 1.0-m concrete border, if present, was unimportant with respect to the measured infiltration rates. Evidence for this assertion can be seen in Fig. 1, which is a contour plot developed from the 256 $S_{L/16}$ measurements. For example, if, as a consequence of lateral divergence of flow below the 1.0-m deep concrete border, a significantly different gradient was present near the plot edges relative to the plot center between the soil surface and a depth of 0.1 m, the depth of infiltrometer installation, then this should result in a greater infiltration rate at the outer periphery of the plot relative to the center. It is clear from Fig. 1 that no such trend was observed.

The results in Table 1 are consistent with the findings of Sisson and Wierenga (1981), who observed a decrease in mean infiltration rate with decreasing measurement scale. The mag-

nitude of the reductions in their study were much less than in our case. We think their observations can be attributed to experimental design. Sisson and Wierenga also used three measurement scales in their study, but the percentage of the total plot sampled at each scale varied between 80% at the largest scale to 3% at the smallest. In contrast, 100% of the 4.0 x 4.0-m plot area was sampled at each scale in our study. Therefore, the mean value at each scale is measured over the same physical area. An "ideal" infiltrometer would measure the mean infiltration rate within the confines of the instrument without altering the actual mean infiltration rate (where "actual" implies the rate that would occur in the absence of the infiltrometer). Since this was not the case, we conclude that the measurement method employed in this study significantly altered the infiltration process during the measurement period. The impact appears to be temporary given the final infiltration rate on the entire plot.

It follows from the smaller scales of observation that even though the mean flow direction was vertical, water movement at the local scale was apparently 3-dimensional. Recent research attempting to define "effective permeabilities" in heterogenous media may provide a theoretical explanation of the observations (Rubin and Gomez-Hernandez 1990; Durlofsky 1992). For example, Durlofsky (1992) generated 2-D random conductivity fields and used numerical flow simulations to calculate "effective block permeabilities" defined relative to the simulation boundary conditions, variance, and spatial correlation scale of conductivities, and the spatial domain represented by the block. He showed that the "effective block permeability" for a heterogenous media is not necessarily a simple arithmetic average of the fine scale permeabilities within the block of interest. Imposing no-flow boundaries for these "spatial blocks," similar to that created by inserting an infiltrometer into the soil, would further alter the block permeability values. We are not aware of these types of numerical simulations in 3-D, which would be appropriate for our experimental conditions. However, our observations of a decreasing mean infiltration rate with decreasing scale of observation may partially be a consequence of this implicit scaling of block permeabilities associated with different scale infiltrometers.

An explanation that is consistent with the variation in the mean infiltration rate as a function of scale is that, in a statistical sense, there is a "stagnation zone" associated with the border of each infiltrometer. The effective width of the stagnation zone is independent of infiltrometer scale and will be denoted by ω (cm). Since the steady-state water flux, Q (cm^3/h), entering each infiltrometer is known, the following formulas give the "adjusted" estimate of the infiltration rate (R,) (cm/h), accounting for a hypothesized stagnation zone. In these formulas, Q_i is the arithmetic average water flux associated with the indicated (i^{th}) scale, given in Table 1.

$$(R,) = \frac{4^2 Q_{L/4}}{A_{L/4}} \quad \text{where } A_{L/4} = 4^2(L/4 - 2\omega)^2 \qquad (2a)$$

$$\langle R_s \rangle = \frac{16^2 Q_{L/16}}{A_{L/16}} \quad \text{where } A_{L/16} = 16^2(L/16 - 2\omega)^2 \qquad (2b)$$

Assuming an ω of 4.0 cm gives a mean infiltration rate for the 4.0 x 4.0-m area of 1.96 cm/h for $S_{L/4}$ and a value of 1.96 cm/h for $S_{L/16}$. These values are in excellent agreement with the measured final infiltration rate of 1.97 cm/h for the same area. Since the concrete border had been in place for over 30 years, no edge effect was assumed for the plot borders. We would emphasize that the assumed value of 4.0 cm for ω is only valid for the mean of the entire plot and does not hold for individual infiltrometers. To illustrate this concept, the adjusted mean value of the infiltration rate for the 0.25 m infiltrometers within each 1.0-m block was computed and compared with the adjusted measured value of the infiltration rate for the corresponding 1.0-m infiltrometer. The correlation coefficient for this comparison was 0.01, suggesting that the reduction in the infiltration rate associated with an individual infiltrometer is quite variable and that the "average" value of this reduction within the entire plot corresponds to a stagnation zone of 4.0 cm.

Based on these calculations, the infiltrometers altered the flow process, on average, in a manner analogous to assuming an apparent stagnation zone adjacent to each infiltrometer edge. However, the impact of inserting an infiltrometer appears to be highly variable for an individual infiltrometer and spatial location, and may even result in an increased infiltration

rate. An additional indication of the variability in the effective stagnation zone is evident in the coefficient of variation (CV) for the adjusted values for scale $S_{L/4}$ (CV = 0.36) and the adjusted mean of the 0.25-m infiltrometers within each 1.0-m block (CV = 0.21).

Spatial variability of observed infiltration rates

The observed spatial variability of the steady-state infiltration is graphically illustrated in Figs. 1 (scale $S_{L/4}$) and 2 (scale $S_{L/16}$). The cumulative frequency distribution is given in Fig. 3. Figure 4 gives the cumulative frequency distribution for the In-transform of the measured infiltration rates. The 16 measurements at scale $S_{L/4}$ provide only a qualitative estimate of the associated probability distribution. However, the 256 observations at scale $S_{L/16}$ provide a sufficient data set for determining the probability distribution. It is evident from these two figures that the lognormal distribution provides a better description of the underlying distribu-

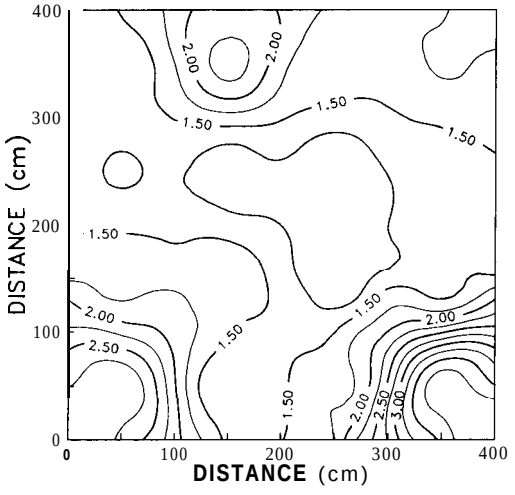

FIG. 1. Spatial distribution of 1.0 x 1.0-m infiltration measurements.

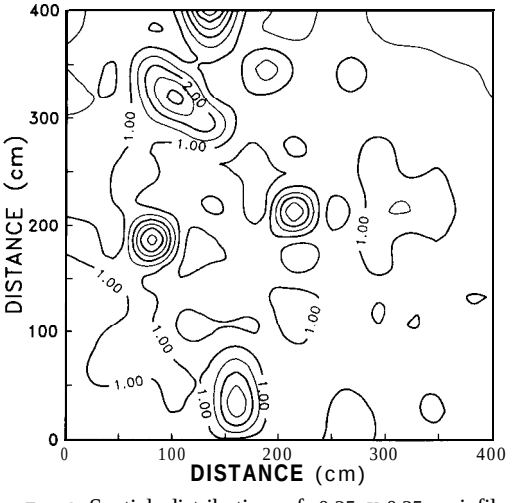

FIG. 2. Spatial distribution of 0.25 X 0.25-m infiltration measurements.

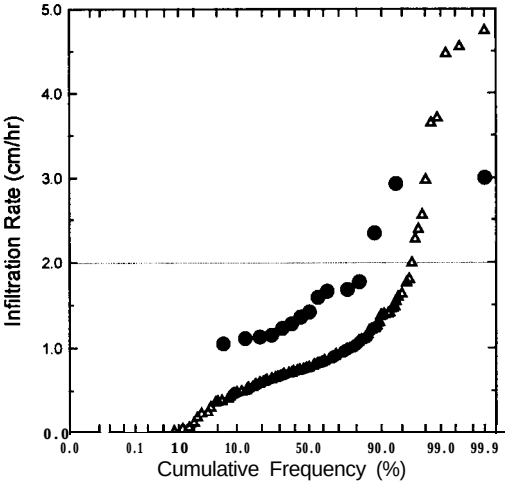

FIG. 3. Cumulative frequency distribution of measured infiltration rates at two instrument scales (● 1.0 X 1.0-m infiltrometer, A 0.25 X 0.25-m infiltrometer).

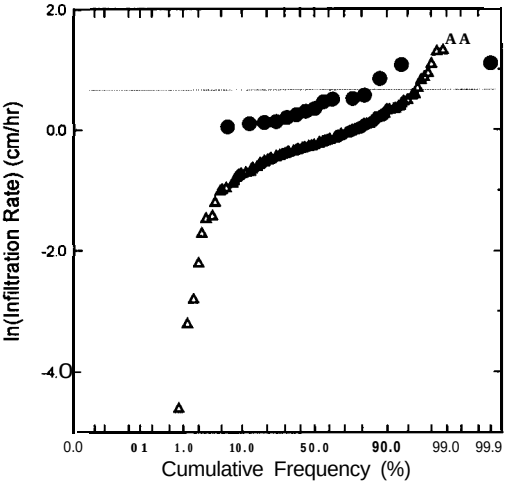

FIG. 4. Cumulative frequency distribution of ln-transformed infiltration rates at two instrument scales (● 1.0 X 1.0-m infiltrometer, A 0.25 X 0.25-m infiltrometer).

tion. This feature was also observed by Vieira et al. (1981) and Sisson and Wierenga (1981). Assuming the infiltration measurements represent realizations of a second-order stationary random function (Journel and Huijbregts 1978) allows us to use additional tools for characterizing the spatial structure.

The measurements at each scale actually represent the mean infiltration rate within the region associated with each infiltrometer. Hence, the measured values are called the *regularization* of the point infiltration rate over this area. The observation that the frequency distribution of the regularized variables at one scale is lognormally distributed does not imply that this is true at any other scale. As pointed out by Journel and Huijbregts (1978), a linear combination of lognormal variables cannot follow a lognormal distribution, although in practice this is sometimes assumed. If one uses the In-transform of the regularized data to compute a semivariogram, this assumption of permanence of lognormality is required in calculating a point semivariogram. Therefore, we chose to work directly with the untransformed infiltration data.

A nonlinear least-squares regression was used to fit the parameters, sill (b), and length scale (x) of an exponential semivariogram model ($\gamma_v(h) = b(1) - \exp(-|h|/\lambda)$) to the experimental regularized variogram, $\gamma_{S_{L/16}}$, of unadjusted infiltration rates at the $S_{L/16}$ scale. This gave the parameters b = 0.374 $(cm/h)^2$ and λ = 14.7 cm. The point semivariogram, r(h), also assumed to be an exponential model, was estimated from the experimental model by deconvolution using the Cauchy-Gauss method and numerical integration as outlined by Journel and Huijbregts (1978). This gave parameter estimates of b = 1.68 $(cm/h)^2$ and λ = 7.0 cm for the point semivariogram (r(h)) and illustrates the influence of regularization on the observed quantity, i.e., reducing the a priori variance (sill) and increasing the correlation length scale. The prediction of $\gamma_{S_{L/16}}$ based on this point semivariogram model can be calculated from the following equation (Journel and Huijbregts 1978).

$$r.(h) = \gamma(v,v_h) - \bar{\gamma}(v,v) \qquad (3)$$

Figure 5a illustrates the theoretical point semivariogram, the calculated experimental semivariogram at scale $S_{L/16}$, and the associated prediction of the regularized semivariogram

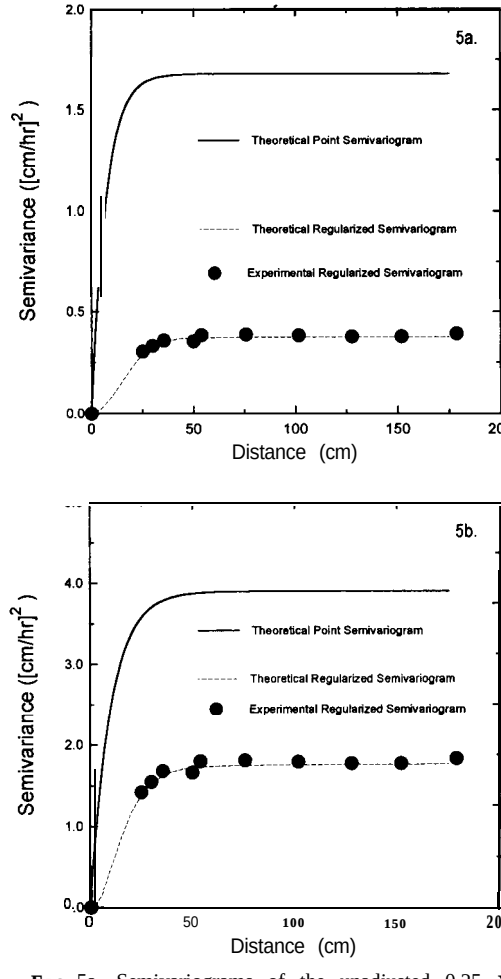

FIG. 5a. Semivariograms of the unadjusted 0.25 X 0.25-m infiltrometer measurements.

FIG. 5b. Semivariograms of the adjusted 0.25 × 0.25-m infiltrometer measurements.

from Eq. (3). As stated above, the actual measured infiltration values, assuming the absence of a stagnation zone, were used in these calculations. However, since the adjusted values differ only by a constant multiplier ($\alpha_{L/16}$ = 625/289), it follows that the adjusted regularized experimental semivariogram should scale as the square of $\alpha_{L/16}$, which thus has a corresponding sill of approximately 4.68 X 0.374 = 1.75 (cm/h)". Using the assumption of a 4-cm stagnation zone and associated measurement scale of 0.17 x 0.17 m, the estimated point semivariogram obtained for the adjusted infiltration rate values by deconvoluting Eq. (3) is $\gamma(h) = 3.9 (- \exp(-|h|/$

10.0)) (Fig. 5b). The point semivariogram, observed experimental, and theoretical regularized semivariograms, assuming the existence of a 4-cm stagnation zone, are given in Fig. 5b. The effective range of the exponential model, defined as the value of h at which $\gamma(h)$ achieves 95% of its maximum value, is approximately 3X. This leads to a range of 0.21 and 0.30 m for the unadjusted and adjusted infiltration rate values, respectively.

Given the point semivariogram, it is straightforward to calculate the expected variance of measurements of any arbitrary shape taken from within any arbitrary finite region. Specifically, the dispersion variance, $D^2(\nu,V)$, gives the expected variance of measurements associated with areas of size ν taken within a region of size V. This variance is given by the following formula.

$$D^2(\nu,V) = \bar{\gamma}(V,V) - \bar{\gamma}(\nu,\nu) \quad (4)$$

Table 2 provides a summary of the observed dispersion variance and that calculated from Eq. (4), with and without assuming a 4-cm stagnation zone, for various combinations of v and V. As noted in the table, the observed experimental variance on the $S_{L/16}$ measurements within regions of V = 0.50 x 0.50 m^2 is 0.235 $(cm/h)^2$ and is lognormally distributed, n = 64 (the variance of the adjusted infiltration rates scales as before: 0.235 x 4.67). The theoretical expectation of this variance computed from Eq. (4) is $D^2(0.25,0.50)_{0.25}$ = 0.233. The corresponding variance for the adjusted infiltration rate values is $D^2(0.17,0.50)_{0.17}$ = 1.19 compared with 1.10, the experimental variance for the adjusted infiltration rates. With these variances being lognormally distributed, neither theoretical value is significantly different from those observed experimentally. For $D^2(0.25,1.00)_{0.25}$ and $D^2(0.17,1.00)_{0.17}$, the theoretical and observed dispersion variances are also in close agreement.

Of more significance are the values of $D^2(1.00, 4.00)_{0.25}$ and $D^2(1.00,4.00)_{0.17}$, which are 0.04 and 0.18 $(cm/h)^2$, respectively. As given in Table 2, the 1 x l-m infiltrometer variance of 0.360 (0.503, adjusted) is significantly different from the predicted values based on the spatial structure estimate for the $S_{L/16}$ measurements. Hence, not only is the mean infiltration estimate biased depending on measurement scale, but the underlying spatial structure/variability is biased as well by the presence of the infiltrometer.

TABLE 2

Dispersion variance analysis, ***giving observed and theoretical variance of measurements of size ν taken within a region of size V***

ν (m)	v (m)	Observed variance ([cm/h]²)	Theoretical variance ([cm/h]²)
0.25	0.50	0.235	0.233
0.25	1.00	0.322	0.331
1.00	4.00	0.360"	0.040
0.17	0.50	1.100	1.190[b]
0.17	1.00	1.510	1.560[b]
1.00	4.00	0.503"	0.180[b]

[a] Calculated from the 16 $S_{L/4}$ measurements.

[b] Expected variance assuming existence of stagnation zone.

CONCLUSIONS

The reason why the mean infiltration rate for a 4.0 x 4.0-m area decreased with decreasing scale of measurement is not clear. One possible explanation is that infiltration is fundamentally a three-dimensional process, and inserting an infiltrometer into the soil disrupts the process near the infiltrometer edges. Infiltrometers apparently impact a significantly larger spatial region than that represented by the volume occupied by the device itself (i.e., the 4-cm average stagnation zone). Tentative supporting evidence for this conclusion was found by examining steady-state infiltration on an adjacent plot (the field site used for this study was subsequently employed in a solute transport experiment in which the plot was destructively sampled). On this one plot, steady-state infiltration was measured after installing the infiltrometer to a depth of 0.05 m. Upon conclusion of this reading, the infiltrometer was "vibrated" to a depth of 0.10 m; the intake rate was then measured and the infiltrometer installed to a depth of 0.125 m. For this single 1.0 x 1.0-m infiltrometer, the effective stagnation zone associated with each depth is illustrated in Fig. 6. Because of the lack of replication, this only serves as a qualitative estimate of the influence of installation depth.

This study suggests that further experimental and theoretical research is required to fully understand the impact infiltrometers have on the infiltration process. For example, work similar to that of Durlofsky (1992) in two dimensions, a three-dimensional numerical simulation of

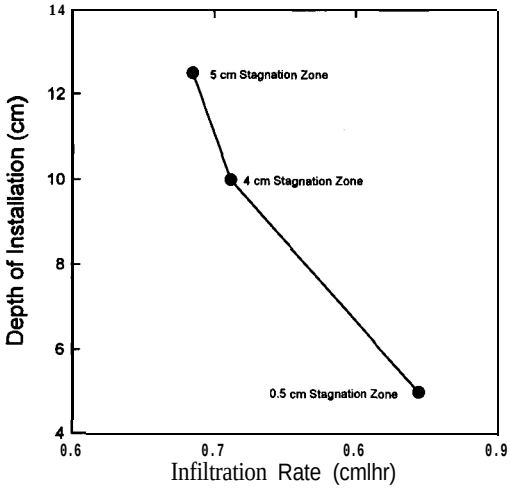

FIG. 6. Effect of infiltrometer installation depth on measured infiltration rate and associated stagnation zone.

steady-state water infiltration into a "soil" with spatially correlated random hydraulic conductivity under imposed "no-flow" borders corresponding to the infiltrometer within a larger simulation region, may help explain the observations and, perhaps, lead to improved measurement methods.

REFERENCES

Bouwer, H. 1986. Intake rate: Cylinder infiltrometer. In Methods of Soil Analysis, part 1. A. Klute (ed.). Monograph 9, American Society of Agronomy, Madison, WI, pp. 825-844.

Clothier, B. E. 1988. Measurement of soil physical properties in the field: Commentary. *In* Flow and transport in the natural environment: Advances and applications. W. L. Steffen and 0. T. Denmead (eds.). Springer Verlag, New York, pp. 86-Y4.

Clothier, B. E., and I. White. 1981. Measurement of sorptivity and soil water diffusivity in the field. Soil Sci. Soc. Am. J. 45:241-245.

Durlofsky, L. J. (1992). Representation of grid block permeability in coarse scale models of randomly heterogeneous porous media. Water Resour Res 28:1791-1800.

Gelhar, L. W., C. Welty, and K. R. Rehfeldt. 1992. A critical review of data on field-scale dispersion in aquifers. Water Resour. Res. 28:1955-1974.

Hess, K. M., S. H. Wolf, and M. A. Celia. 1992. Large-scale natural gradient tracer test in sand and gravel, Cape Cod, Massachusetts, 3. Hydraulic conductivity variability and calculated macrodispersivities. Water Resour. Res. 28:2011-2027.

Journel, A., and Ch. J. Huijbregts. 1978. Mining Geostatistics. Academic Press, London.

Jury, W. A. 1985. Spatial variability of soil physical parameters in solute migration. A critical literature review. Rep. EPRI EA-4228, Elec. Power Res. Inst., Palo Alto, CA.

Lauren, J. G., R. J. Wagenet, J. Bouma, and J. H. M. Wosten. 1988. Variability of saturated hydraulic conductivity in a Glossaquic Hapludalf with macropores. Soil Sci. 145:20-28.

Rubin, Y., and J. J. Gomez-Hernandez. 1988. A stochastic approach to the problem of upscaling of conductivity in disordered media: Theory and unconditioned numerical simulations. Water Resour. Res. 26:691-701.

Sisson, J. B., and P. J. Wierenga. 1981. Spatial variability of steady-state infiltration rates as a stochastic process. Soil Sci. Soc. Am. J. 45:699-704.

Sposito, G. 1986. The "physics" of soil physics. Water Resour. Res. 22:835-885.

Vieira, S. R., D. R. Nielsen, and J. W. Biggar. 1981. Spatial variability of field-measured infiltration rate. Soil Sci. Soc Am. J. 45:1040-1048.

White, I. 1988. Measurement of soil physical properties in the field. *In* Flow and Transport in the Natural Environment: Advances and Applications. W. L. Steffen and 0. T. Denmead (eds.). Springer Verlag, New York, pp. 59-85.

Zobeck, T. M., N. R. Fausey, and N. S. Al-Hamdan. 1985. Effect of sample cross-sectional area on saturated hydraulic conductivity in two structured clay soils. Trans. **ASAE** 28:791-794.